Journal of Applied Polymer Science

Transcrystallinity and relevant interfacial strength induced by carbon nanotube fibers in a polypropylene matrix

Yao Gao,[1] Yi Wu,[1] Maoqing Liang,[1] Qiang Fu[2]

[1]Department of Material Engineering, Zhejiang Industry and Trade Vocational College, Wenzhou 325003, China

[2]State Key Laboratory of Polymer Materials Engineering, College of Polymer Science and Engineering, Sichuan University, Chengdu 610065, China

Correspondence to: Y. Gao (E-mail: yaogao83@163.com) and Q. Fu (E-mail: qiangfu@scu.edu.cn)

ABSTRACT: For polymer composites, interfacial crystalline structures retain an important role in the macroscopic properties and are significantly affected by the processing conditions, such as the temperature, time, and external field. In this study, the transcrystallization behavior of the carbon nanotube fiber and isotactic polypropylene composite was investigated by polarizing light microscopy. The influence of the formation of the transcrystalline layer on the interfacial adhesion was evaluated by a single-fiber fragmentation test. The results show that the growth rate of the transcrystalline layer was strongly influenced by the isothermal crystallization temperature, and the interfacial shear strength was markedly enhanced by the formation of the layer. The interfacial adhesion was further increased with the gradual perfection and growth of transcrystallinity. © 2015 Wiley Periodicals, Inc. J. Appl. Polym. Sci. **2015**, *132*, 42119.

KEYWORDS: composites; crystallization; polyolefins

Received 14 September 2014; accepted 20 February 2015
DOI: 10.1002/app.42119

INTRODUCTION

Fiber-reinforced polymer composites have aroused much attention and have been widely applied. Generally, the mechanical properties of fiber-reinforced polymer composites not only depend on the properties of the fibers and polymer matrix, but they also depend on the interfacial adhesion between the fibers and the matrix. In semicrystalline polymer composites, the fibers can act as orientation templates for polymer crystallization.[1–5] When the fiber nucleates the crystallization of the polymer with its massive nuclei, the restricted development of the spherulites occurs, and the crystal grows unidirectionally normal to the fiber axis. As a result, an oriented polymer crystalline layer known as a transcrystalline layer (TCL; transcrystallinity) develops close to the fiber surface. The transcrystalline (TC) structure is a well-known interfacial crystalline structure in polymer–fiber systems, and it arouses much attention not only because of this unique crystalline morphology but also because this interfacial crystalline structure produces a higher Young's modulus than the bulk spherulites.[6,7] More importantly, some researchers have reported that the TCL could increase the interfacial adhesion and enhance the load-transfer efficiency from the polymer matrix to the fibers.[8,9] However, other works revealed that it had no or even negative effects on the interfacial adhesion between the fibers and the matrix.[10,11] Ogata *et al.*[12] found that the bond strength of the composite was not affected by the formation of the TCL. Folkes and Wong[11] even proved that the reduction of the interfacial shear strength (IFSS) occurred by transcrystallization. Therefore, how and to what extent the TCL influences the interfacial adhesion of the polymer composite still needs investigation to draw some more convincing conclusions.

Carbon nanotubes (CNTs) possess unique structures and excellent mechanical properties[13–18] and, thus, are regarded as preferred reinforcing fillers to prepare composite materials with high mechanical properties.[19–22] However, many results have shown that the reinforcing effect of CNTs was at least two orders of magnitude lower than the value predicted according to relevant composite theory as the results of highly entangled and randomly oriented CNTs.[23–25] Therefore, fabrication macroscopic assemblies of CNTs have become one method for taking advantage of the excellent properties of CNTs at the macroscopic level. Recently, carbon nanotube fibers (CNTFs), as macroscopic assembles of individual CNTs, have been considered to have great potential for constructing advanced composites because of their light weight and multiple functionalities.[26–28] Moreover, it has been reported that the highest tensile strength of CNTFs could reach 9 GPa; this surpasses the values of most conventional fibrous materials.[29] All of these make CNTFs another ideal reinforcing agent for polymer composites. In CNTF-reinforced polymer composites, CNTFs were reported to

be good nucleation agents for polymer matrixes. Zhang *et al.*[30] provided evidence of the TCL around CNTFs by means of polarized optical microscopy and scanning electron microscopy (SEM). Zhang *et al.*[31] also showed that the TC lamellae could bridge the adjacent aligned nanotube bundles after melting recrystallization. Here, an intriguing question was raised: will the formation of a TCL affect the interfacial adhesion between the matrix and CNTFs and how can we characterize such an influence in a convincible way?

In this study, CNTFs were incorporated into an isotactic polypropylene (iPP) matrix to prepare single-fiber-reinforced composite specimens. The interfacial crystallization behavior at the fiber surface was investigated with the aid of polarized optical microscopy. The evolution of iPP transcrystallization at different isothermal crystallization temperatures was studied. Moreover, the IFSS of the composite was determined with a single-fiber fragmentation (SFF) test, and the variation of the IFSS during the development of the TCL was revealed in a quantitative way. Our results demonstrate that the interfacial crystallization could be an effective physical way to enhance the interfacial adhesion of integrated CNTF composites.

EXPERIMENTAL

Materials

iPP was supplied by Dushanzi Petroleum Chemical Incorporation (Xinjiang, China) and had a weight-average molecular weight of 39.9 $\times$ 10^4 g/mol and a weight-average molecular weight/number-average molecular weight ratio of 4.6.

The CNTFs, with a diameter of 22 μm, were supplied by the Physics Department of Tsinghua University.

CNTF Tensile Test

The tensile strength of a single CNTF was performed on an electronic single-fiber strength tester (LLY-06ED) with a 200-cN load cell. The gauge length was 10 mm, and the crosshead speed used was 10 mm/min. The tensile strength (δ_f) of each CNTF was calculated according to the following formula:

$$\delta_f = 4F/\pi d^2$$

where F is the broken force and d is the diameter of the CNTF. The final fragmentation strength (508 MPa) was calculated as an average value of 30 CNTFs.

SFF Test

A single CNTF was fixed between two iPP sheets with the same thickness and hot-pressed at 200°C under 5 MPa for 5 min. Then, the sample was rapidly removed to another vulcanizing machine to crystallize isothermally at 134°C for 0, 1, 3, 5, and 9 min. All of the crystallized specimens were then quenched in ice water (ca. 0°C) to maintain the crystalline structure. Finally, the specimens were cut into dumbbell-shape samples, and during the cutting, the CNTF had to be in the center position of each sample.

The SFF test was conducted on an Intron 5567 universal testing machine with a 100-N load cell at a crosshead speed of 5 mm/min at room temperature (23 $\pm$ 2°C). The tested samples were then observed with an optical microscope to obtain the fragmentation length and the diameter of the CNTF. The IFSS was calculated according to eqs. (1) and (2):[32,33]

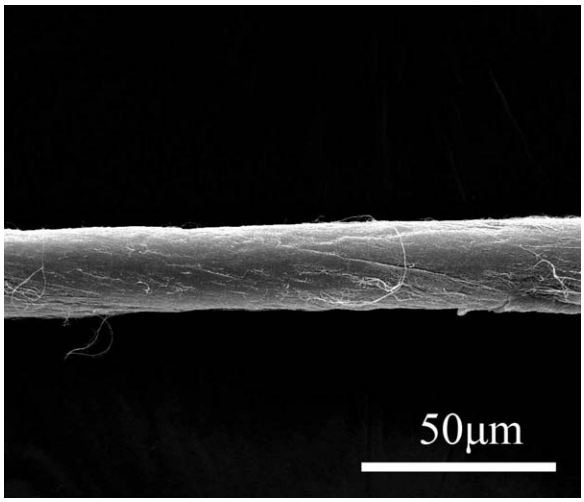

Figure 1. SEM image of the morphology of the CNTF.

$$\tau = \frac{\delta_f}{2l_c} d_f \quad (1)$$

where τ is the IFSS, δ_f is the tensile strength of the CNTF, d_f is the diameter, and l_c is the critical effective length of CNTF. The fragmentation length is related to l_c and is generally between $2/l_c \approx l_c$, and the average fragmentation length ($\bar{l}$) of the fiber can be expressed as Kl_c, where K is the correction factor for random orientation of the fibers and is always 0.75.[34] Therefore, eq. (1) can be modified as follows:

$$\tau = \frac{3\delta_f d_f}{8\bar{l}} \quad (2)$$

The IFSS value for each situation was calculated as the average of at least five samples.

Polarizing Light Microscopy

The transcrystallization behavior in the iPP/CNTF composite was observed with a polarizing light microscope equipped with a hot-stage. The methods of sample preparation and characterization were as follows: one piece of iPP film with a CNTF in the center between two microscope glass slides was first heated to 200°C at a heating rate of 50°C/min, maintained for 5 min to erase the previous thermal history, and then cooled down to the expected isothermal temperature (i.e., 126, 128, 130, 132, 134, 136, 138, and 140°C, respectively). We recorded the isothermal crystallization morphology of the specimens by taking photographs with a digital camera at a certain intervals.

SEM

The CNTF and related samples were observed by an FEI Inspect F scanning electron microscope at an acceleration voltage of 20KV. The morphology of the CNTF characterized by SEM is shown in Figure 1. To characterize the crystallization structure of the samples, the single-fiber-based composites were first cryogenically fractured in liquid nitrogen and then etched for 1 h in a solution containing 1.3 wt % potassium permanganate, 32.9 wt % concentrated sulfuric acid, and 65.8 wt %

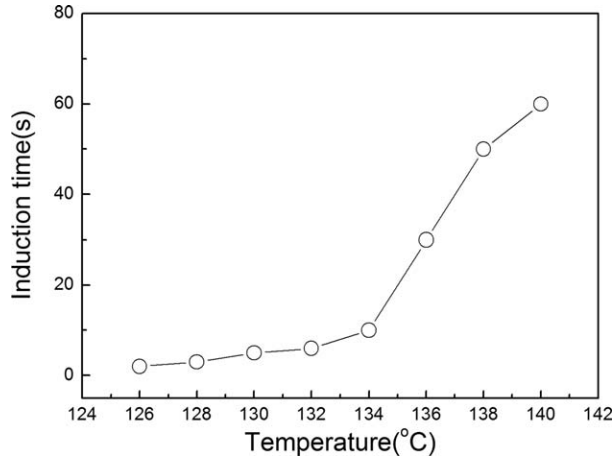

Figure 2. Induction time of the transcrystallinity versus the crystallization temperature.

concentrated phosphoric acid, according to the procedure proposed by Olley and Bassett.[35]

RESULTS AND DISCUSSION

Transcrystallization Behavior in the iPP/CNTF Composite

Transcrystallites are one of the typical crystalline structures in fiber-reinforced iPP composites. In this study, the transcrystallization behavior in the iPP/CNTF composite was first observed by polarizing light microscopy. The curve of the induction time (onset time for the occurrence of transcrystallization) of iPP versus the crystallization temperature in this study is shown in Figure 2. It was obvious that the induction time of the iPP matrix became longer when the crystallization temperature escalated. In particular, when the isothermal crystallization was set over 134°C, the relevant induction time changed dramatically. For examples, the induction time was 6 s at 132°C and 30 s at 136°C. Two factors contributed to such a phenomenon. First, the lower the crystallization temperature was, the bigger the supercooling degree was, and the improved supercooling was favorable for the nucleation of the iPP matrix. Second, the higher crystallization temperature gave birth to a higher ability of thermal motion of the iPP polymer chains, and the random thermal motion was unfavorable for the nucleation of the iPP matrix. Under the combined effect of these two factors, the nucleation of the iPP matrix happened quickly at a relatively lower crystallization temperature; this led to a short induction time. When the crystallization temperature was higher than 134°C, the effect of the thermal motion of the iPP chain was dominant, and this dramatically prolonged the induction time.

Figure 3(a) reveals the relationship between the crystallization time and the thickness of the interfacial transcrystallinity in the iPP/CNTF composite. To better identify the relationship, Figure 4(b) was plotted according to the slope coefficients (which represent the growth rates of the transcrystallinity) of the lines in Figure 3(a) against the related crystallization temperatures. Clearly, from Figure 3(a,b), it was clear that the interfacial transcrytalline layer in iPP/CNTF was strongly dependent on the crystallization temperature and time. The growth rate of the

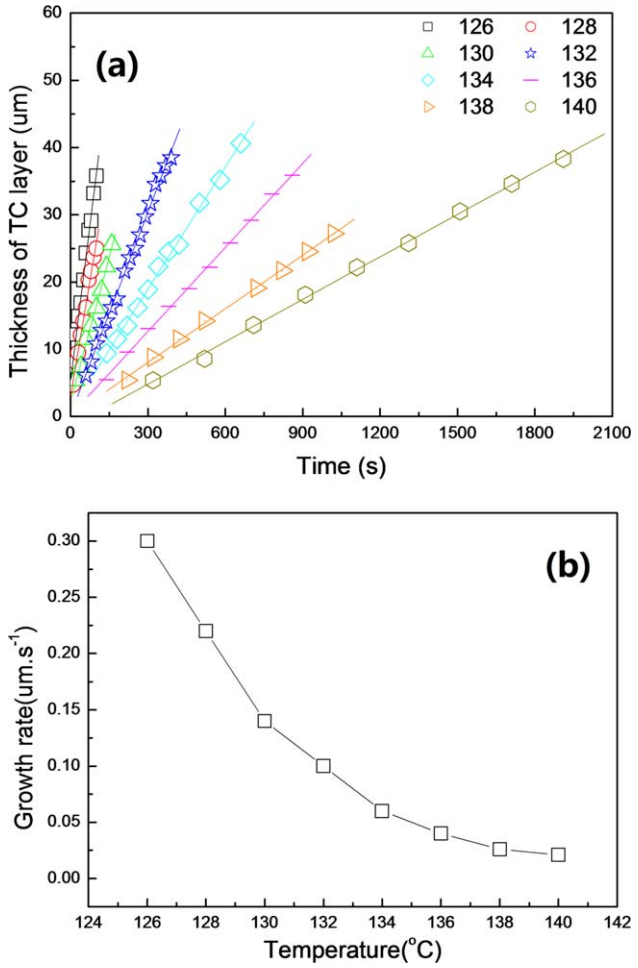

Figure 3. (a) Transcrystal thickness versus the crystallization time for the iPP/CNTF microcomposite and (b) growth rate of the transcrystal versus the crystallization temperature. [Color figure can be viewed in the online issue, which is available at wileyonlinelibrary.com.]

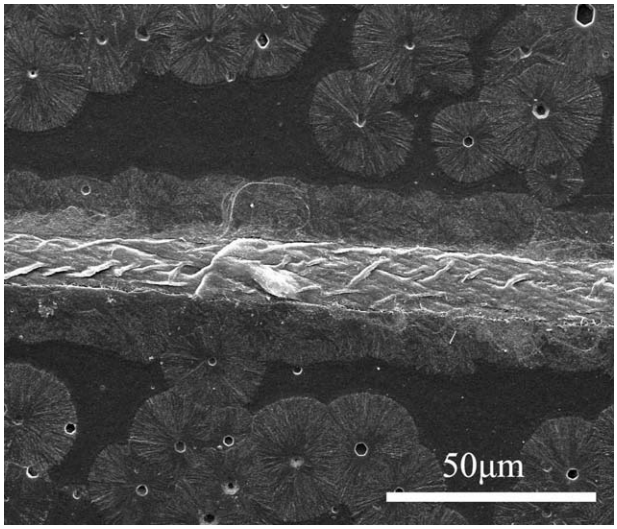

Figure 4. SEM image of the typical crystallization morphology of the iPP/CNTF composite.

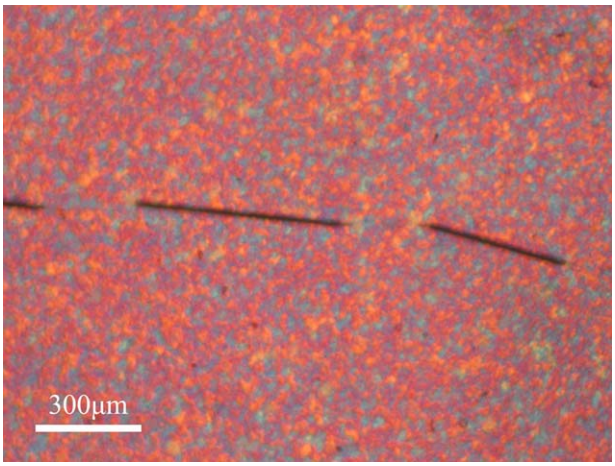

Figure 5. Typical fractured CNTF morphology in the iPP matrix. [Color figure can be viewed in the online issue, which is available at wileyonlinelibrary.com.]

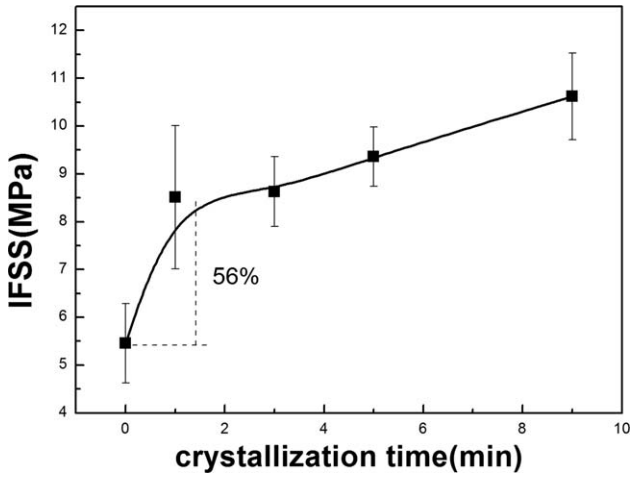

Figure 6. IFSS of the iPP/CNTF composite versus the crystallization time.

transcrystallinity decreased when the crystallization temperature increased.

Relationship Between the Transcrytallinity and Interfacial Adhesion

For most TC structures in fiber-reinforced polymer composites, the *c* axis of the lamellae is parallel to the longitudinal direction of the fibers; this means that the lamellae are perpendicular to the fibers. Such an oriented crystalline structure can influence the interfacial adhesion between the fibers and matrix of the composites. To obtain the actual interfacial crystalline structure of the iPP/CNTF composites manufactured by molding, we first observed the mixed-acid etched sample with SEM, as shown in Figure 4. This iPP/CNTF sample was molded at 134°C for 5 min and then quickly quenched in cold water (~0°C). The SEM image in Figure 4 shows the existence of TCL in this iPP/CNTF composite. As shown in Figure 4, the CNF was in the middle of the image, and the compacted TCL was at the interface between the CNTF and iPP matrix. Furthermore, some iPP spherulites were also observed as the main crystal structure of the PP matrix away from the CNTF. In addition, we also found that there was no obvious detachment at the interface even when the sample was etched by the strong mixed acid; this, in some way, indicated good interfacial adhesion between the iPP matrix and CNTF in the existence of the TCL.

For accurate measurement of the interfacial adhesion of iPP/CNTF and an in-depth discussion of the relationship between the interfacial adhesion and the formation of the transcrystallinity, the SFF was used to obtain the exact values of the IFSS of the composite, as SFF is one of the most widely used micromechanical testing methods for quantitatively assessing the interfacial adhesion.

Figure 5 is a typical polarizing light microscopy observation image of the fractured CNTF after the composite sample was stretched to necking on an Instron 5567 universal testing machine. One can clearly see that the CNTF was fractured into several shorter pieces. It is easy to imagine, during the stretching process, that the load transferred into the CNTF through the iPP-CNTF interface. The CNTF could not help to share the load until the load transferred onto the CNTF reached or exceeded its ultimate tensile strength, and as a result of this overload of the stretching force, the CNTF was fractured into short parts. The fractured short parts could then continue sharing the load until they were fractured into even shorter parts. Such a process kept happening until the CNTF fragments were too short to share the load or the load transferred from the interface was too weak to break the short pieces of the CNTF. Each of these two mechanisms could stop the CNTF from fracturing; this means that the fracture of the CNTF reached a saturation point. According to eq. (2), the IFSS of the iPP/CNTF composites corresponding to different crystallization times is shown in Figure 6.

For the sample with no interfacial crystallization, in which case the sample was not isothermally crystallized but quickly quenched, the IFSS value was 5.45 MPa. In contrast, when iPP/CNTF was isothermally crystallized for 1 min, the IFSS value of the sample reached 8.5 MPa with a 56% increase. Figure 6 tells us that the prolonging of the crystallization time helped to increase the IFSS values of the composites. In the experimental range, when the crystallization time reached 9 min, the composite possessed an IFSS of 10.6 MPa. In conclusion, the formation of the transcrystallinity in the iPP/CNFT composites was favorable to the enhancement of the IFSS, and the transcrystallinity could be perfected and thickened by the prolonging of the crystallization time; this resulted in a higher IFSS value. It could be imagined that the iPP polymer chains were induced to form the partially ordered structure (the precursor of a nucleus) on the surface of the CNTF because of its heterogeneous nucleating effect. Along with the formation of the nuclei and the growth of the crystals, the crystallization around the CNTF produced interface contraction, and the interface contraction led to shrinkage stress at the interface. The shrinkage stress dispersed on the atomic scale and forced these ordered PP chains to wrap the CNTF with a certain interfacial adhesion. Meanwhile, this certain interfacial adhesion was consolidated by the formation of the TCL. Therefore, a special composite filler was formed: CNTF inside, wrapped with transcrystallinity. The outside of

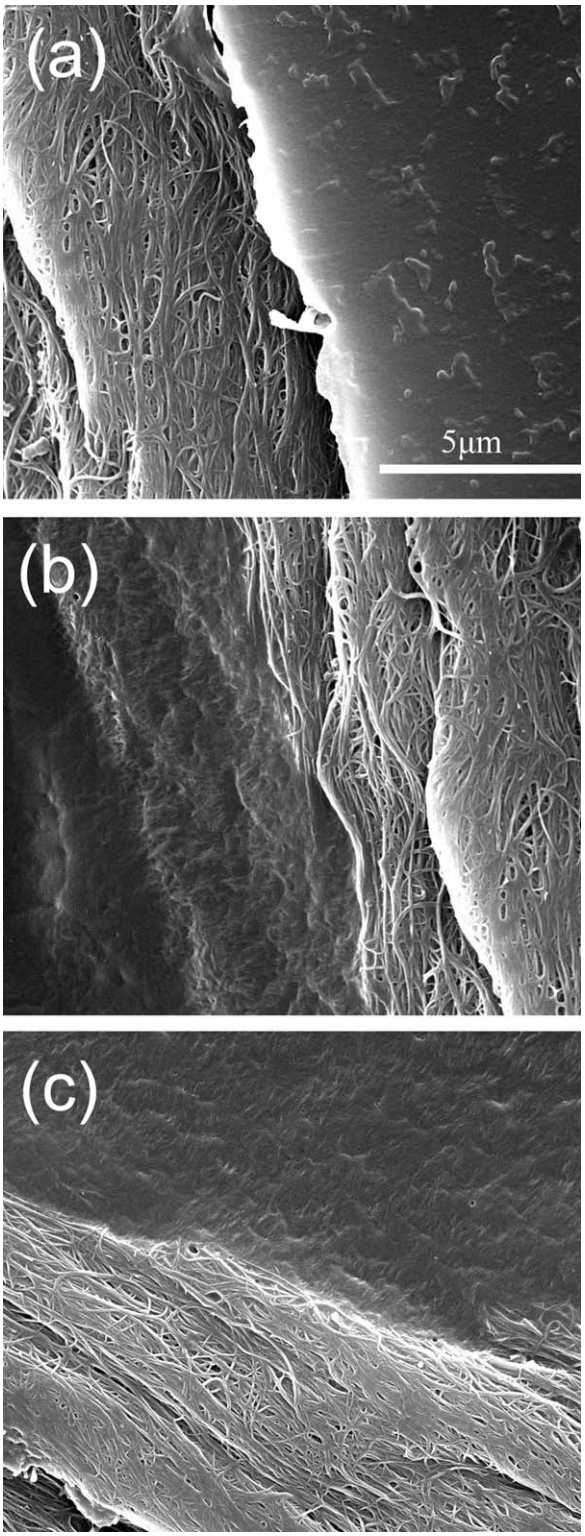

Figure 7. SEM images of the typical interface of the iPP/CNTF composite isothermally crystallized at 134°C for (a) 0, (b) 1, and (c) 3 min.

this composite filler was totally compatible with the iPP matrix and could transfer the load/stress in a highly efficient way. So, the wrappage around the CNTF (i.e., the TCL) was a critical factor in determining the relative IFSS value. A greater crystallization time meant a thicker transcrystallinity (wrappage) and more perfect crystals; this increased the interfacial adhesion between the iPP matrix and CNTF and led to a higher IFSS value.

It is reasonable to believe that the increased IFSS value was related to the well-bonded interfacial adhesion induced by transcrystallization. Therefore, different interfaces of the samples after isothermal crystallization in the hot-stage for different times were observed via SEM (as shown in Figure 7). As shown in Figure 7(a), debonding occurred at the interface of the quenched iPP and CNTF sample. In contrast, the interfacial adhesion between iPP and CNTF was clearly better after isothermal crystallization for 1 and 3 min [Figure 7(b,c)]; this indicated that the TC layers could bring good interfacial adhesion between the polymer matrix and CNTF. This result was consistent with the results of the IFSS test in some way.

CONCLUSIONS

In this study, the interfacial crystallization behavior of single-CNTF/iPP composites was investigated. Transcrystallinity was successfully induced by the CNTF in the iPP matrix, and the induction time and growth rate of the transcrystallinity at the CNTF–iPP interface strongly depended on the crystallization temperature. The increased crystallization temperature caused a longer induction time and lower growth rate of the transcrystallinity. The results from SFP testing show that the formation of the transcrystallinity at the interface between the iPP matrix and CNTF remarkably improved the IFSS value. This effect occurred even in the early stage of transcrystallization and was amplified with the perfection and thickening of the transcrystallinity. The results of SFP testing and the interfacial morphology observation strongly suggest that the interfacial adhesion between the CNTF and iPP matrix was enhanced by the formation of the TCL and such an effect was further strengthened by the thickening and perfecting of the transcrystallinity. This provides an effective physical way to enhance the interfacial adhesion in CNTF-based composites.

ACKNOWLEDGMENTS

The authors express their sincere thanks to the Department of Education of Zhejiang Province [Study on Achieving High-Performance Environmentally Friendly Poly(L-lactide); Y201432352 (2014)] and Wenzhou Science and Technology (contract grant number G20140004) for their financial support.

REFERENCES

1. Liang, Y. Y.; Liu, S. Y.; Dai, K.; Wang, B.; Shao, C. G.; Zhang, Q. X.; Wang, S. J.; Zheng, G. Q.; Liu, C. T.; Chen, J. B.; Shen, C. Y.; Li, Q.; Peng, X. F. *Colloid Polym. Sci.* **2012**, *290*, 1157.
2. Wang, C.; Liu, F. H.; Huang, W. H. *Polymer* **2011**, *52*, 1326.
3. Wang, Y. M.; Tong, B. B.; Hou, S.; Li, M.; Shen, C. Y. *Compos. A* **2011**, *42*, 66.
4. Wang, K.; Guo, M.; Zhao, D.; Zhang, Q.; Du, R.; Fu, Q. *Polymer* **2006**, *47*, 8374.

5. Ning, N. Y.; Zhang, W.; Yan, J. J.; Xu, F.; Wang, T. N.; Su, H.; Tang, C. Y.; Fu, Q. *Polymer* **2013**, *54*, 303.
6. Kewi, T. K.; Schonhorn, H.; Frisch, H. L. *J. Appl. Phys.* **1967**, *38*, 2512.
7. Hata, T.; Ohsaka, K.; Yamada, T.; Nakamae, K.; Shibata, N.; Matsumoto, T. *J. Adhes.* **1994**, *45*, 125.
8. Heppenstall-Butler, M.; Bannister, D. J.; Young, R. *J. Compos. A* **1996**, *27*, 833.
9. Gao, S. L.; Kim, J. K. *Compos. A* **2000**, *31*, 517.
10. Gati, A.; Wagner, H. D. *Macromolecules* **1997**, *30*, 3933.
11. Folkes, M. J.; Wong, W. K. *Polymer* **1987**, *28*, 1309.
12. Ogata, N.; Yasumoto, H.; Yamasaki, K.; Yu, H.; Ogihara, T.; Yanagawa, T. *J. Mater. Sci.* **1992**, 27, 5108.
13. Iijima, S. *Nature* **1991**, *354*, 56.
14. Coleman, J. N.; Blau, W. J.; Dalton, A. B.; Munoz, E.; Collins, S.; Kim, B. G.; Razal, J.; Selvidge, M.; Vieiro, G.; Baughman, R. H. *Appl. Phys. Lett.* **2003**, *82*, 1682.
15. Treacy, M. M. J.; Ebbesen, T. W.; Gibson, J. M. *Nature* **1996**, *381*, 678.
16. Kilbride, B. E.; Coleman, J. N.; Fraysse, J.; Fournet, P.; Cadek, M.; Drury, A. *J. Appl. Phys.* **2002**, *92*, 4024.
17. Koysuren, O.; Karaman, M.; Ozyurt, D. *J. Appl. Polym. Sci.* **2013**, *127*, 4557.
18. Baughman, R. H.; Zakhidov, A. A.; de Heer, W. A. *Science* **2002**, *297*, 787.
19. Kearns, J. C.; Shambaugh, R. L. *J. Appl. Polym. Sci.* **2002**, *86*, 2079.
20. Chang, T. E.; Jensen, L. R.; Kisliuk, A.; Pipes, R. B. *Polymer* **2005**, *46*, 439.
21. Jose, M. V.; Dean, D.; Tyner, J.; Price, G.; Nyairo, E. *J. Appl. Polym. Sci.* **2007**, *103*, 3844.
22. Manchado, M. A. L.; Valentini, L.; Biagiotti, J.; Kenny, J. M. *Carbon* **2005**, *43*, 1499.
23. Wang, Z.; Liang, Z.; Wang, B.; Zhang, C.; Kramer, L. *Compos. A* **2004**, *35*, 1225.
24. Gou, J. *Polym. Int.* **2006**, *55*, 1283.
25. Coleman, J. N.; Blau, W. J.; Dalton, A. B.; Munoz, E.; Collins, S.; Kim, B. G.; Razal, J.; Selvidge, M.; Vieiro, G.; Baughman, R. H. *Appl. Phys. Lett.* **2003**, *82*, 1682.
26. Gao, Y.; Li, J.; Liu, L.; Ma, W.; Zhou, W.; Xie, S.; Zhang, Z. *Adv. Funct. Mater.* **2010**, *20*, 3797.
27. Zhang, S. J.; Koziol, K. K. K.; Kinloch, I. A.; Windle, A. H. *Small* **2008**, *4*, 1217.
28. Xiao, L.; Liu, P.; Liu, L.; Jiang, K.; Feng, X. F.; Wei, Y.; Qian, L.; Fan, S. S.; Zhang, T. H. *Appl. Phys. Lett.* **2008**, *92*, 3.
29. Koziol, K.; Vilatela, J.; Moisala, A.; Motta, M.; Cunniff, P.; Sennett, M.; Windle, A. *Science* **2007**, *318*, 1892.
30. Zhang, S.; Minus, M. L.; Zhu, L.; Wong, C. P.; Kumar, S. *Polymer* **2008**, *49*, 1356.
31. Zhang, S.; Lin, W.; Wong, C. P.; Bucknall, D. G.; Kumar, S. *ACS Appl. Mater. Intell.* **2010**, *2*, 1642.
32. Kelly, A.; Tyson, W. R. *J. Mech. Phys. Solids* **1965**, *13*, 329.
33. Awal, A.; Cescutti, G.; Ghosh, S. B.; Muessig, J. *Compos. A* **2011**, *42*, 50.
34. Schaefer, J. D.; Rodriguez, A. J.; Guzman, M. E.; Lim, C. S.; Minaie, B. *Carbon* **2011**, *49*, 2750.
35. Olley, R. H.; Bassett, D. C. *Polymer* **1982**, 2, 1707.